Anomalous diffusion in non-Markovian walks having amnestically induced persistence

A. S. Ferreira,[1] J. C. Cressoni,[1] G. M. Viswanathan,[2] and Marco Antonio Alves da Silva[3]
[1]*Instituto de Física, Universidade Federal de Alagoas, Maceió 57072-970, AL, Brazil*
[2]*Consortium of the Americas for Interdisciplinary Science and Department of Physics and Astronomy, University of New Mexico, Albuquerque, New Mexico 87131, USA*
[3]*Universidade de São Paulo, 14040-903 Ribeirão Preto, SP, Brazil*
(Received 3 August 2009; published 19 January 2010)

We report numerically and analytically estimated values for the Hurst exponent for a recently proposed non-Markovian walk characterized by amnestically induced persistence. These results are consistent with earlier studies showing that log-periodic oscillations arise only for large memory losses of the recent past. We also report numerical estimates of the Hurst exponent for non-Markovian walks with diluted memory. Finally, we study walks with a fractal memory of the past for a Thue-Morse and Fibonacci memory patterns. These results are interpreted and discussed in the context of the necessary and sufficient conditions for the central limit theorem to hold.

DOI: 10.1103/PhysRevE.81.011125 PACS number(s): 05.40.Fb

I. INTRODUCTION

Random walks are ubiquitous in the literature because of their applications to modeling a large variety of natural or human induced phenomena. They particularly are important in the study of phenomena that display log-periodicity, which is a main point of this work, and may appear, for example, in economic crashes and earthquakes [1]. In the models presented here, log-periodicity appears because of the loss of recent memory, what we termed amnestic effect. A variety of diffusive systems, from particles going through porous media up to epidemics and also ideas (or information) may present memory with gaps. Therefore, we introduced random walks with memory gaps or, what we called "memory dilution," in order to simulate these systems. We verified that all these memory effects may cause anomalous diffusion with similar behaviors.

Before the pioneering and revolutionary contributions of Paul Lévy [2], the conventional wisdom held that the central limit theorem (CLT) remained valid for most if not all stochastic processes. Therefore, alternatives to Gaussian distributions and normal diffusion, characterized by mean squared displacement scaling linearly with time, did not draw much attention or captivate the imagination of scientists. The central limit theorem holds, under certain conditions, that sums of N random variables follow a Gaussian distribution in the limit of large N. There are three important conditions for the CLT to hold true: (i) independence of the random variables, (ii) finite variances of each random variable, and a lesser known axiom (iii) the variances of each random variable divided by the variance of the sums must converge to zero for $N \to \infty$. Anomalous diffusion and Lévy statistics become relevant when one or more conditions fail. We briefly examine these possibilities. Violation of condition (iii) leads to the somewhat expected—if not trivial—result that the sum becomes dominated by those terms whose variance does not contribute infinitesimally to the sum. Violations of condition (ii) lead to a generalization of the CLT and the skew Lévy α-stable distribution takes on the role of the Gaussian distribution. The focus of our work represents the breakdown of condition (ii) above, which we further explore through a phase diagram analysis.

Without loss of generalization and in order to render the discussion more relevant, let us consider time series. What happens to the sum x of N consecutive elements of such series when condition (ii) fails? If the random variables fail to meet the condition of statistical independence, then this implies the existence of correlations in the series of random variables. We can categorize correlations as either, having short range, i.e., a finite correlation time or length exists beyond which the variables become essentially statistically independent, or long range, in which case the correlations decay as power laws. Power laws $f(x) \sim x^{\alpha}$ have no characteristic scale in the sense that a scale transformation leaves the power-law intact: $f(\lambda x) \sim f(x)\lambda^{\alpha}$. Short-range correlations correspond to Markov processes and therefore a renormalization by an appropriate scale leads to a recovery of normal diffusion, since the CLT becomes valid.

On the other hand, long-range correlations imply underlying non-Markovian processes. No scale transformation can guarantee an elimination of the correlations or a recovery of normal diffusion. A number of situations can arise. On the one hand, the sums of the random variables might still converge to a Gaussian distribution, but the variance might not grow linearly with N. This corresponds to fractional Brownian motion. The mean squared displacement scales as

$$\langle x^2 \rangle \sim N^{2H}, \tag{1}$$

but now the Hurst exponent H no longer equals 1/2. Superdiffusion corresponds to $H > 1/2$ and subdiffusion to $H < 1/2$. Another possibility is that the correlations prevent convergence to any distribution whatsoever, i.e., the stability property (e.g., Lévy stability, or Gaussian stability) disappears.

In this context, the recently proposed model of a non-Markovian walk and its exact solution have revealed new mechanisms by which correlations and memory can disrupt the behavior expected from the CLT. The unexpected surprise concerned how loss of memory can, in fact, increase the Hurst exponent. In the next section, we review the model

and summarize the methodology. In Sec. III we report our numerical results, interpret and discuss them and finally in Sec. IV we provide concluding remarks.

II. MODEL AND METHODS

We have adapted [3] a novel approach introduced by Schütz and Trimper [4] for studying walks with long-range memory [5–8], for studying memory loss. For the sake of completeness, we repeat here some results obtained in Ref. [9], and get new analytical results for the second moment and correlations.

Consider the iterative procedure to calculating the position of a random walker,

$$x_{t+1} = x_t + v_{t+1}, \tag{2}$$

where $v_t = \pm 1$. Through the generation of random numbers with uniform distribution, we randomly select at time t, a previous time $1 \le t' < ft$ $(0 \le f \le 1)$. Thus, one chooses the current step direction v_t based on the value of $v_{t'}$, using the following rule: the walker repeats the action taken at time t' with probability p, and with probability $1-p$ the walker goes in the opposite direction $-v_{t'}$. Without generality loss, we fix the first step direction to the right, i.e., $v_1 = +1$.

Now, starting at $t=0$, let the memory range be $L \equiv \text{int}(ft)+1$, where int$(x)$ denotes the integer part of x, for $0 \le f < 1$ ($L=t$ for $f=1$). We could write an expected value for v_{t+1} as $v^e_{t+1} = \alpha \frac{x_L - x_0}{L}$, where $\alpha = 2p-1$. Thus, considering $x_0 = 0$, we find the following differential equation for the first moment in the asymptotic limit (see Ref. [9] for details):

$$\frac{d}{dt}\langle x_t \rangle = \frac{\alpha}{ft}\langle x_{ft} \rangle. \tag{3}$$

Using an expansion in the form $\langle x_t \rangle = \Sigma_i A_i t^{\delta_i} \sin(B_i \ln(t) + C_i)$ in Eq. (3), we obtain a system of transcendental equations linking B and δ given by

$$\delta = \alpha f^{\delta-1} \cos(B \ln f) \tag{4}$$

$$B = \alpha f^{\delta-1} \sin(B \ln f). \tag{5}$$

We analyze now the possible solutions for the system. For $\alpha < 0$, there exists oscillating solutions with a threshold defined by a continuous set of values (p, f). Consider the case without oscillations ($B=0$). Thus, Eq. (4) reduces to

$$\delta = \alpha f^{\delta-1}, \tag{6}$$

which has solutions only for $f > f_0(p)$. Kenkre [10] obtained the critical line for the onset of log-periodicity given by

$$-\alpha \ln(1/f_0) = f_0/e, \tag{7}$$

represented by a dashed line in Fig. 1(a). Using the Lambert W function (see Appendix), we find an alternative proof for Eq. (7).

For $\alpha \ge 0$, Eq. (4) has a maximum value of δ for $B=0$, which also satisfies Eq. (5). As the term with the largest δ dominates in any expansion, thus $B=0$ should govern the long term behavior. In agreement with this prediction, we find no oscillations in our simulations (not shown). Note that for the ballistic case ($p=1$) the solution $(B, \delta) = (0, 1)$ is exact for any f. For $\alpha \ne 0$ and $\delta > 1/2$ we obtain superdiffusion, but log-periodicity only exists for $\alpha < 0$, as we will see below along with the analysis of the second moment.

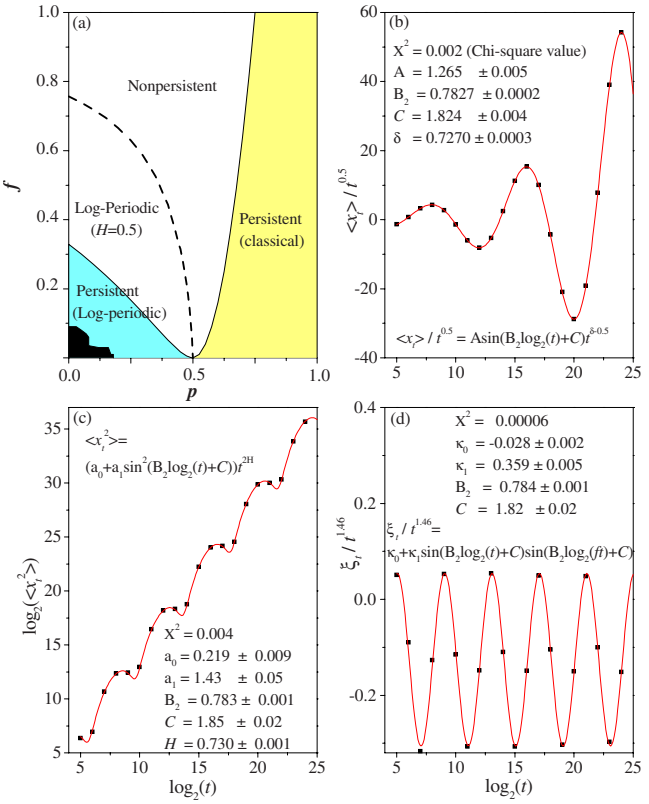

FIG. 1. (Color online) (a) Complete phase diagram showing the four phases [9], plotted according to the exact solutions given by Eqs. (11) and (21). The dashed line $f_0(p)$ delineates the threshold for log-periodicity and cleaves the nonpersistent regime into two [Eq. (7)]. The dark region represents numerical results with $H \gtrsim 0.85$, having strong log-periodicity, because a_0 and κ_0 are small in this region. (b), (c), and (d) show first, second moments and correlation, respectively, for $p=0.1$ and $f=0.15$. We normalized the first moment by $t^{0.5}$ and the correlation by t^{2H}, while was taken the logarithm of the second moment to the base two. Points represent the simulations and continuous lines fittings with the functions shown. The total number of steps (maximum time) was 16 777 216, and the number of runs was 5000 to obtain the averages. We can easily verify the relations (16) and (17) in the text. Note the consistency between the parameters $B_2 = B\ln(2)$, C and H, because the fittings were accomplished independently; also, we can verify that $H = \delta$ considering the precision of the numbers.

Next, we study the solutions of the differential equation for the second moment:

$$\frac{d}{dt}\langle x_t^2 \rangle = 1 + \frac{2\alpha}{ft}\xi(t), \tag{8}$$

where $\xi(t) = \langle x_t x_{ft} \rangle$ represents the correlation between the position at time t and that one at the end of the memory range. As $|\langle x \rangle| \le (\langle x^2 \rangle)^{1/2}$, follows that there exists a function $F(t)$ such that

$$\xi(t) = F(t)(\langle x_t^2\rangle\langle x_{ft}^2\rangle)^{1/2}, \tag{9}$$

with $-1 \le F(t) \le 1$.

For $\alpha > 0$ $(p > 1/2)$ the oscillations disappear, and $F(t \to \infty) = 1$. Thus, we can show that, asymptotically, the transcendental relationship for the Hurst exponent is

$$H = \alpha f^{H-1}. \tag{10}$$

This result corresponds to Eq. (6) with $\delta = H$. For $H = 1/2$, we obtain the curve

$$f = 16\left(p - \frac{1}{2}\right)^2, \tag{11}$$

that separates the diffusive and anomalous regions for $p \ge 1/2$ in the plane (p,f) [see Fig. 1(a)]. The case $f=1$ gives $p_c = 3/4$, in agreement with Ref. [4].

For $\alpha \le 0$, we follow a different (more complete and detailed) approach from that one used in our recent work [9]. We write the following series expansions to the second moment and correlation:

$$\langle x_t^2\rangle = \sum_{i=0}^{\infty} a_i \sin^2[b_i \ln(t) + c_i] t^{2H_i}; \tag{12}$$

$$\xi(t) = \sum_{i=0}^{\infty} \kappa_i \sin[b_i \ln(t) + c_i]\sin[b_i \ln(ft) + c_i] t^{2H_i}. \tag{13}$$

For the case $f=1$, we have $\xi(t) = \langle x_t^2\rangle$ leading to $\kappa_i = a_i$ and $b_i = 0$, thus recovering the full memory result. Another simple condition with an exact result happens for $\alpha = 0$ $(p = \frac{1}{2})$, from which we trivially obtain $\langle x_t^2\rangle = t$. We can then write $x_t = x_{ft} + \Delta x_t$ which gives $\xi(t) = \langle x_{ft}^2\rangle + \langle x_{ft}\Delta x_t\rangle$. However, since in this case x_{ft} and Δx_t, are independent random variables, we have $\langle x_{ft}\Delta x_t\rangle = \langle x_{ft}\rangle\langle \Delta x_t\rangle = 0$. Therefore $\xi(t) = \langle x_{ft}^2\rangle$ that gives $\xi(t) = ft$, from which follows $a_i = \kappa_i = 0$ for $i \ne 0$, $a_0 \sin(c_0) = 1$, $b_0 = 0$, $\kappa_0 = f$, $H_0 = \frac{1}{2}$, and from Eq. (9) we obtain $F(t) = f^{1/2}$. Note that $F(t) = 1$ only for $f = 1$, showing a discontinuity for this function with the parameter α for $f \ne 1$.

Through simulation experiments we could find that the main contributions for the leading terms of the second moment and correlation are given by

$$\langle x_t^2\rangle \sim \{a_0 + a_1 \sin^2[b_1 \ln(t) + c_1]\} t^{2H}, \tag{14}$$

$$\xi(t) \sim \{\kappa_0 + \kappa_1 \sin[b_1 \ln(t) + c_1]\sin[b_1 \ln(ft) + c_1]\} t^{2H}. \tag{15}$$

Numerical simulations have shown that for $H \gtrsim 0.85$, there exists a region in the plane f vs p where a_0 and κ_0 are negligible. The moments and correlations oscillate with large amplitudes [strong log-periodicity—see small dark area in Fig. 1(a)], in agreement with results of our recent work [9]; as we approach of the critical line, the terms $a_0 t^{2H_0}$ and $\kappa_0 t^{2H_0}$, and higher-order terms in the expansions become important. Exactly on the critical line, we obtain a marginally superdiffusive solution: $\langle x_t^2\rangle \sim \{a_0 + a_1 \sin^2[b_1 \ln(t) + c_1]\} t \ln(t)$ and $\xi(t) \sim \{\kappa_0 + \kappa_1 \sin[b_1 \ln(t) + c_1]\sin[b_1 \ln(ft) + c_1]\} t \ln(t)$.

Using the relations (14), (15), and (9), we can show that

$$\kappa_1 = a_1 f^H \tag{16}$$

for the case $\kappa_0 = a_0 = 0$; however, based on results from simulations (see Figs. 1(b)–1(d) as an example) we assume that this is a general result.

For $2H > 1$, substituting Eqs. (14) and (15) in Eq. (8), we obtain

$$a_0 = \frac{\alpha\kappa_0}{Hf}, \tag{17}$$

$$H = \alpha f^{H-1} \cos(b_1 \ln f), \tag{18}$$

$$b_1 = \alpha f^{H-1} \sin(b_1 \ln f). \tag{19}$$

We assume that the dominant terms of $\langle x_t\rangle$ and $\langle x_t^2\rangle$ have the same "period" and phase difference, so that $b_1 = B$ and $c_1 = C$. Thus, the Eqs. (4) and (5) turn out to be identical to the Eqs. (18) and (19); therefore, we obtain the expected relation $H = \delta$. Indeed we conjecture that for walks lacking subdiffusion, $\delta \ge 1/2$ always implies $H = \delta$. This result was first conjectured based on exact results for $f = 1$, but now we rigorously proved for $f < 1$, a quite general model without subdiffusion. This seems to hold for any anomalous diffusion, although a general proof is still lacking. However, we can do the following approach: for a ballistic motion we have $H = \delta$ trivially; so, assuming that this result is valid for a motion nearly ballistic is reasonable, i.e., with a Hurst exponent given by $H = \delta = 1 - \epsilon$, with ϵ very small. Thus, by inductive reasoning we can conclude that this may be true up to the transition line. For values of f greater than f_c, i.e., above the critical line we have $\kappa_1 = a_1 = 0$ and $a_0 = 1 + 2\frac{\alpha}{f}\kappa_0$. Thus, the relations (18) and (19) are not valid anymore, and H turns out equal to 1/2. For $\delta < 1/2$ we have that $H > \delta$, showing how important are the fluctuations and the higher moments, besides raising questions about possible multifractal scaling [11]. From Eqs. (18) and (19), without loss of generality, by choosing the positive root we obtain: $B = (\alpha^2 f^{2H-2} - H^2)^{1/2}$, and $B/H = \tan[B \ln(f)]$ what leads to the expression

$$H \tan[\ln(f)\sqrt{\alpha^2 f^{2H-2} - H^2}] = \sqrt{\alpha^2 f^{2H-2} - H^2} \tag{20}$$

for $\delta \ge 1/2$ and $H = 1/2$ otherwise; obviously the correct H values must give positive radicands. The solution of Eq. (20) with $H = \delta = 1/2$ corresponds to the separation line of the diffusive and anomalous phases [see Fig. 1(a)] given by

$$2\sqrt{\frac{\alpha_c^2}{f_c} - \frac{1}{4}} = \tan\left[\ln(f_c)\sqrt{\frac{\alpha_c^2}{f_c} - \frac{1}{4}}\right]. \tag{21}$$

At $p = 0$, we obtain the critical value of $f_c(0) = 0.3284$ for the onset of log-periodic superdiffusion. We note that $(p_c, f_c) = (1/2, 0)$ represents a multicritical point. Thus, the onset of superdiffusion represents a second, smoother, phase transition. All phase transitions together yield a total of four different phases.

Now, we discuss the particular case of constant memory range L that has a trivial, ballistic solution in the asymptotic limit for $p \ne 1/2$. The equation for the first moment is $\frac{d}{dt}\langle x_t\rangle = \frac{\alpha}{L}\langle x_L\rangle$, which gives $\langle x_t\rangle \sim At$, where $A = \frac{\alpha}{L}\langle x_L\rangle$ is con-

stant. This is sufficient to conclude that the diffusion is ballistic, however, it is interesting to analyze the second moment: $\frac{d}{dt}\langle x_t^2\rangle = 1 + \frac{2\alpha}{L}\langle x_L x_t\rangle$. As L is fixed, in the limit $t \to \infty$, x_L and x_t become uncorrelated variables, thus, for finite but very large t we can write $\langle x_L x_t\rangle \sim \langle x_L\rangle\langle x_t\rangle$. Therefore, we obtain $\langle x_t^2\rangle \sim (At)^2 = \langle x_t\rangle^2$, i.e., $H=\delta=1$; note that this result is valid also for $f=0$ $(L=1)$.

To generalize still more the model, we introduced different memory profiles, i.e., different distributions of points for the walker to remember inside the memory range given by $L=ft$. We, thus, introduced the dilution idea (represented by d), i.e., the walker remembers only part of the total number of steps given in the time interval $[0,L]$.

We accomplished three types of dilutions: (1) random, (2) Thue Morse [12], and (3) Fibonacci. In the first memory profile with dilution some points inside the interval $[0,L]$ are chosen randomly and they are cleaned from the memory; in the dilution $d=0.1$, for instance, one erases 10% of the memory. Particularly, for $d=0$ the model reduces to the initial model without dilution; $d=1$ is the case totally without memory, i.e., the walker does not remember of any point.

For the second profile, we adopted the binary Thue Morse's sequence, generated by the substitutions: $0 \to 01$ and $1 \to 10$, beginning with 1, giving: $T = 1101001100101101001011 0\ldots$, where the sequence is temporal, and one turns the memory off in the time position that the digit is zero.

Finally, the third profile, was the Fibonacci sequence, generated by the rule $T(n+1)=T(n)+T(n-1)$, being $T(1)=0$ and $T(2)=1$ the first two Fibonacci numbers. Thus, we store the v_T values in the memory, of the steps taken at instants of time: $T=1-2-3-5-8-13-21\ldots$; so, we can only remember the actions taken at time instants belonging to this sequence. We can easily see that the dilution causes a walk with an *effective* memory range $L^*=(1-d)L$.

In the following, we describe the main motivations for the choice of these three protocols. Random dilution is a pattern of facile use to control the densities of remembered points, and it is a simple example of a pattern stochastically generated. The other two are examples of nonrandom patterns; the first one, Thue-Morse is equivalent to a dilution of 50% intended to represent nonrandom middle and the second one, the Fibonacci, very high dilutions. Additionally, these sequences are ubiquitous, appearing everywhere, from nature to computers (memory allocation).

To analyze the behavior of the random walks, besides the moments, another important quantity is the persistence length w, that here we defined as the number of steps given by the walker in the same direction until the point that the walker turns back. The distribution of the persistence lengths identifies the types of regimes: Gaussian and non-Gaussian. Normal diffusions have Gaussian propagators, so they present exponential persistence length distributions, whereas anomalous diffusion may present nonexponential distributions (e.g., Lévy walks present power-law tailed persistence length distributions). When anomalous diffusions have Gaussian propagators, we expect that they will present exponential persistence length distributions. In the next section we show the results and discussion.

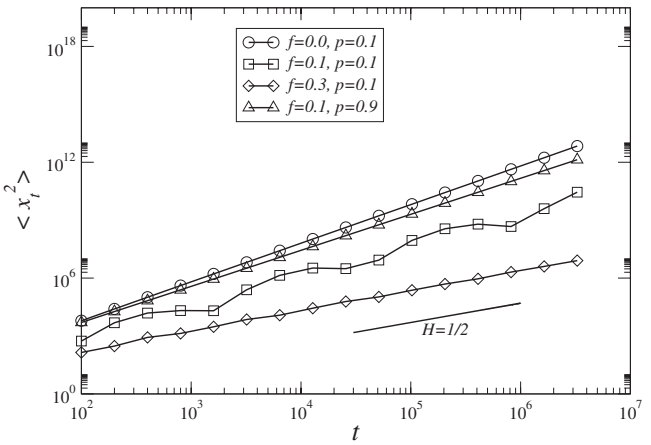

FIG. 2. Much loss of memory (except $f=0$) and small values of p, drives to large oscillations to the second moment. For small values of f, the walker tends to go far away, but his (or her) walk is dampened for small values of p, that does the walker prefer to make the opposite of what he (or she) did in a past time, causing oscillations to the moments. Observe that oscillations do not exist for $f=0.1$ and $p=0.9$, the walker will always want to do what he (or she) did in the past, without so much indecision. Averages were accomplished with 1000 runs reaching 3 276 800 total time units each.

III. NUMERICAL RESULTS AND DISCUSSION

We accomplished many simulations with several f and p parameters, but here we present only those that are relevant to our analysis. For the figures from 2 to 5 we analyze results for the model without dilution.

In Fig. 2 we see the behavior of the second moment with the time t showing log-periodicity for small values of f. The cause of the oscillations is because the walker always tries to do the opposite of his action taken in a distant past [3]. Now, in Figs. 3(a) and 3(b) we plot the position of the walker as a function of time, with a clear display of log-periodicity. In Fig. 3(b) we see the effect amplified through the normalization of the position with the traditional random walk scale without correlations. In Fig. 4 we plot H versus f. We see that for $p > 0.5 + \sqrt{f_c}/4$ [see Eq. (11)] and $f < f_c$ the walker always has superdiffusive behavior. Thus, the threshold for the parameter p is $p=0.75$ $(f_c=1)$, starting from where the behavior of the walker is always superdiffusive for any value of f. For $p<0.5$, the line that separates normal diffusion from anomalous diffusion is given by the solution of the transcendental Eq. (21). The discrepancies shown in Fig. 4, between theoretical values and simulations, are due to convergence difficulties generated by the long-range memory in areas close to areas of phase change or to the critical point $p_c=0.75$.

In Fig. 5, we show the Hurst exponent versus p for several values of f. For any f (except $f=0$) a critical value for p exists, starting from where the walker becomes superdiffusive [see the expressions (11) and (21)]; for $f=0$, normal diffusion only happens at $p=1/2$. What was truly unexpected, was the finding of superdiffusive behavior within the negative feedback region $(p<1/2)$. We clearly see the onset of superdiffusion at a critical value of f persisting all the way down to $f=0$, even for $p<1/2$. In this region the behavior of

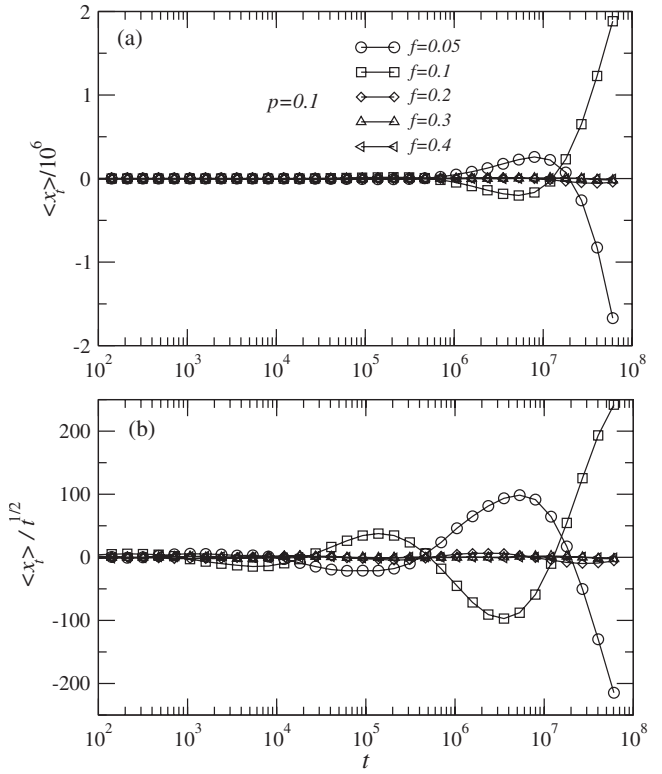

FIG. 3. (a) a semilog plot of the displacement $\langle x_t \rangle$ as function of time for $p=0.1$, and several values of f. (b) Shows with details that big losses of recent memories (small values of f) drive to large amplitudes of variation of position and large log-periodic oscillations.

the walker becomes log-periodic, and we cannot eliminate the correlations with same behavior that appear, through renormalization, or by any scale transformation. For $f=1$ the model reduces to the model of Schütz and Trimper [4] for which the critical point happens at $p=3/4$ where the walker becomes superdiffusive.

Starting to analyze the more general memory profile models, we notice in Fig. 6 that the dilution did not affect qualitatively the results when compared with those of undiluted memory, shown in Fig. 5. In Fig. 7 we show the Hurst exponent for several values of f and d; notice that the scaling behavior might be the same for all dilutions. The small changes observed should be due to finite size effects, i.e., size of the system and size of the sample of independent walks used for the average.

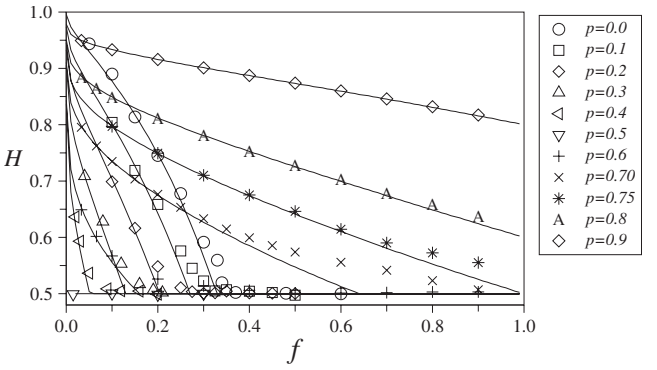

FIG. 4. This figure shows a plot of H versus f (fraction of the old memory), for several values of p. Here analytical results are also shown (full lines) and numeric (symbols). For $p<0.75$ two regimes are possible, according to f: normal diffusion ($H=0.5$) and superdiffusive ($H>0.5$). For $p\geq 0.75$ exists only superdiffusive behavior (for $p=0.75$ and $f=1$ is marginally superdiffusive), for any value of f. Averages were accomplished with 1000 runs and 3 276 800 total time units each.

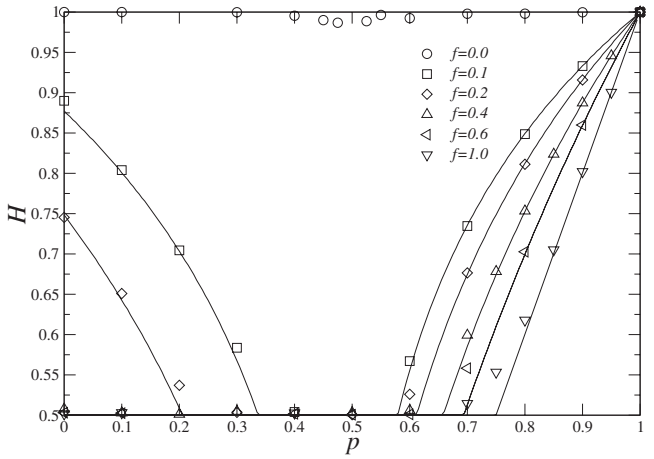

FIG. 5. This figure shows the Hurst exponent H versus p, the probability of the walker to accept the decision taken at time t' $(0<t'<t)$. The symbols represent the results of the simulations, while the full lines represent the analytical results; 1000 runs were accomplished for several values of f for the walker that forgot $(1-f)t$ of the recent past, for a total time of 3 276 800 steps. For the case $f=0$, the walker does not remember anything, except the first step; his (or her) behavior is superdiffusive, except to $p=0.5$, where the exponent H drops abruptly to 0.5, according to the exact result. For small values of f (0.1 and 0.2), even for $p<0.5$, we can see persistence ($H>0.5$). For $f=1.0$ (full memory) we have the well known analytical case showing a good correlation with the simulations; the persistent region just appears for $p>3/4$. Overall, we can see a good correlation between the analytical results and the numerical ones.

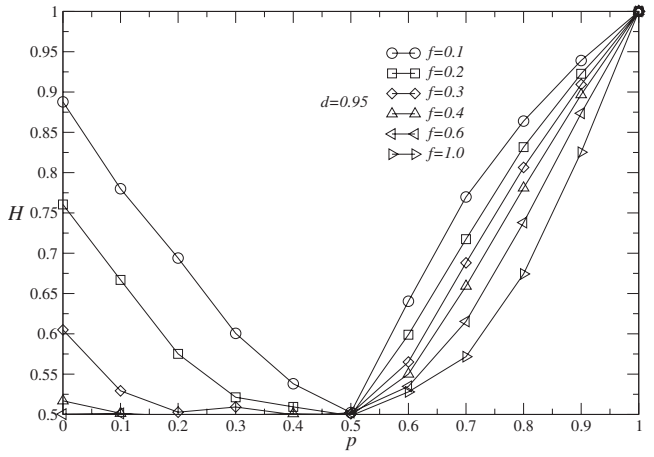

FIG. 6. H versus p plot. The addition of vacancies (dilution) in the total memory of the walker did not provide significant changes in the Hurst exponent. For a dilution of 95% ($d=0.95$) and several f values, the results obtained are almost equivalent to the zero dilution. The critical case happens for $d=1.0$ (totally diluted memory), in which the walker just reminds the first step, equivalent to $f=0.0$ (no dilution case).

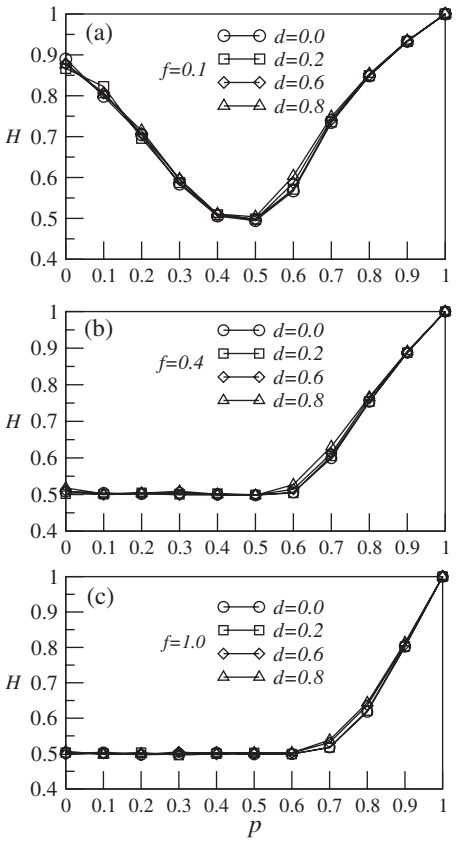

FIG. 7. This figure shows Hurst exponent H against p for several f: (a) $f=0.1$, (b) $f=0.4$, (c) $f=1.0$, and several random dilutions. We can compare the case without dilution ($d=0.0$) with $d=0.2$, 0.6 and 0.8 to conclude that larger dilutions just may cause a small increase in H when $p>0.5$; however, the results might be biased by finite size effects, so the curves might be collapsed. Averages were accomplished with 1000 runs and 3 276 800 total time units each.

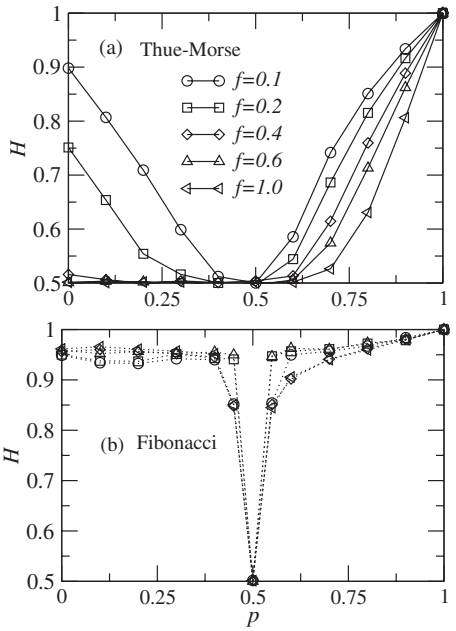

FIG. 8. This figure shows the inclusion of predefined memory to the walker, (a) satisfying the sequence of Thue-Morse that is equivalent to a dilution of 50%. (b) The Fibonacci sequence, where each time given by the number of the sequence corresponds to a point of the memory accessible to be remembered. For the total time of 3 276 800 steps, using the sequence of Fibonacci, only 33 more localized positions of memory exist in the initial instants, what is equal to a dilution close to 100%. We can see that the position of the memory seems not to have any relevance in the Hurst exponent. Averages were accomplished with 1000 runs and 3 276 800 total time units each.

We show in Fig. 8(a) the Hurst exponents for the Thue Morse profile memory with a dilution $d=0.5$; the changes in the results were not significant when compared with a random dilution with $d=0.95$ (Fig. 6). In Fig. 8(b) we see results for H using the Fibonacci sequence that corresponds to a dilution close to 100%. Overall we did not notice any significant influence resulting from the tested diluted memory profiles in the scaling behavior of the system. The reason for this fact is argued in the next paragraph.

Finally, we analyze the persistence shown in the Fig. 9 for two cases of dilution: without ($d=0.0$) and high dilution ($d=0.95$) for some values of p with $f=1.0$ (classic case) and $f=0.1$. We scaled the persistence lengths by an averaged value. In Figs. 9(a) and 9(b), we see the case without dilution. For $f=1.0$ the curves collapse with good precision, while for $f=0.1$, we have deviations from the exponential distribution for small values of p. One can see in the Figs. 9(c) and 9(d), the cases with dilution, not differing appreciably from the results seen in the Figs. 9(a) and 9(b), without dilution. We may understand these similarities through the effective step direction, which depends essentially on the number of steps taken in the forward and backward directions at the used memory; this is so because of the uniform random search of the points with memory. In fact, for example, the probability to take a decision to give a step forward in an instant $t+1$ of a single walk with the *effective* memory range $L^* \leq L$ is $n_f(L^*)/L^*$; therefore, the decision depends only of the *coarse-grained* probability of the considered event, not of its detailed distribution. This argument could also explain the same system scale behavior for different memory profiles. Further studies are needed to complete and clarify this hypothesis.

IV. CONCLUDING REMARKS

The rich phase diagram showed in Fig. 1(a) obtained for this solvable non-Markovian random walk model is rather surprising. An expected lack of Gaussian behavior is unusual, which happens only for small f and p as seen in Figs. 9(b) and 9(d). Even so, the breakdown of the CLT caused by the memory loss can be found in two regions shown in Fig. 1(a), but just one of them ($\alpha>0$) presents Gaussian behavior. Another important finding was a totally unexpected appearance of persistence in a region with negative feedback ($\alpha<0$), which only occurs for large memory losses (low values of f) of the recent past. This provides a direct link between system behavior and damages in the recent memory, namely that, damages in the recent memory can lead to system's persistence behavior in the long time limit. Because of

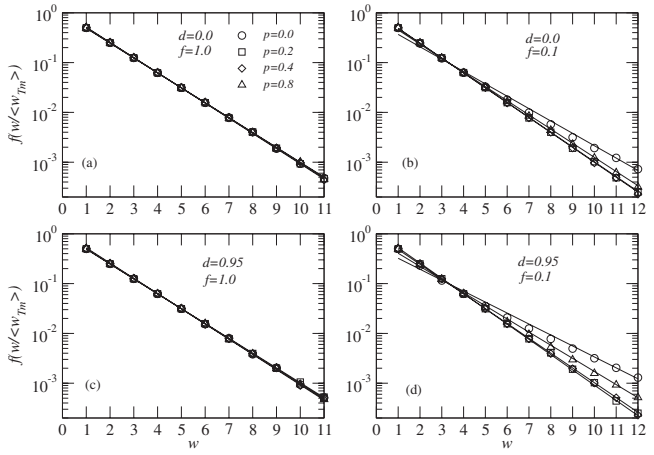

FIG. 9. This figure shows that the distribution of persistence lengths (normalized by the average), typically follows an exponential distribution. In (a), $f=1.0$, the data collapses in a single straight line, showing no appreciable variation in the inclination with different values of p. In (b), $f=0.1$, we note a significant deviation from exponential distribution to $p=0.0$. In (c) and (d), we see that the inclusion of a dilution of 95% did not affect the distributions significantly. Averages were accomplished with 1000 runs and 1 000 000 total time units each.

recent memory loss, we have earlier termed this effect as amnestically induced persistence. Discrete scale invariance (DSI) appears in the region of log-periodicity. The Hurst exponent shows a superdiffusive behavior in the region with order parameter $B \neq 0$. This result is very important in the study of several interesting phenomena (e.g., biological and economic phenomena).

ACKNOWLEDGMENTS

We thank the anonymous referees for the criticisms and suggestions that helped to substantially improve the quality of the paper. We acknowledge CAPES, CNPq (Process Grant No. 201809/2007-9) and FAPESP (Grant No. 2007/04220-4) for funding and Annibal Figueredo and Iram M. Gléria for discussions.

APPENDIX: LAMBERT W FUNCTION

We define the multivalued LambertW function as the inverse of the function,

$$g(W) = W \exp(W). \tag{A1}$$

Let us define the variable $y=-\ln(f)$, f being the fraction that defines the effective memory length. Starting with Eq. (6) of the main text, $\delta=\alpha f^{\delta-1}$, for $\alpha<0$, by taking the natural logarithm of both sides and isolating $-\ln(f)$, we obtain

$$y = \frac{1}{1+|\delta|}\ln\left(\frac{|\delta|}{|\alpha|}\right). \tag{A2}$$

By defining $x=\frac{|\delta|}{|\alpha|}$, we get

$$y = \frac{1}{1+|\alpha|x}\ln(x). \tag{A3}$$

Observe that this function is defined only for $y \leq y_c$ such that y_c is an extremum (maximum). We can obtain such a critical point with the first derivative of y, given

$$y_c = \text{LambertW}\left(\frac{1}{e|\alpha|}\right).$$

Therefore, $\frac{1}{e|\alpha|}=y_c \exp(y_c)$. However, $y_c=-\ln(f_0)$, thus, $\frac{1}{e|\alpha|}=-f_0^{-1}\ln(f_0)$, or equivalently,

$$-\alpha \ln(1/f_0) = f_0/e, \tag{A4}$$

what is the mentioned equation obtained by Kenkre [4]. Curiously, we can write the solution f_0 for the above equation as

$$f_0 = e|\alpha|\text{LambertW}\left(\frac{1}{e|\alpha|}\right). \tag{A5}$$

[1] S. Gluzman and D. Sornette, Phys. Rev. E **65**, 036142 (2002).
[2] P. Levy, *Theorie de l'addition des Variables Aleatoires* (Gauthier-Villars, Paris, 1937).
[3] J. C. Cressoni, Marco Antonio Alves da Silva, and G. M. Viswanathan, Phys. Rev. Lett. **98**, 070603 (2007).
[4] G. M. Schütz and S. Trimper, Phys. Rev. E **70**, 045101(R) (2004).
[5] R. Metzler and J. Klafter, Phys. Rep. **339**, 1 (2000).
[6] R. Metzler and J. Klafter, J. Phys. A **37**, R161 (2004).
[7] V. M. Kenkre, in *Statistical Mechanics and Statistical Methods in Theory and Application*, edited by U. Landman (Plenum, New York, 1977).
[8] V. M. Kenkre, E. W. Montroll, and M. F. Shlesinger, J. Stat. Phys. **9**, 45 (1973).
[9] Marco Antonio Alves da Silva, G. M. Viswanathan, A. S. Ferreira, and J. C. Cressoni, Phys. Rev. E **77**, 040101(R) (2008).
[10] V. M. Kenkre, e-print arXiv:0708.0034.
[11] M. L. Felisberto, F. S. Passos, A. S. Ferreira, M. A. A. da Silva, J. C. Cressoni, and G. M. Viswanathan, Eur. Phys. J. B **72**, 427 (2009).
[12] F. Iglói, L. Turban, and H. Rieger, Phys. Rev. E **59**, 1465 (1999).